

# Autophagic program is regulated by miR-325

L Bo<sup>1,4</sup>, D Su-Ling<sup>1,4</sup>, L Fang<sup>1,4</sup>, Z Lu-Yu<sup>1</sup>, A Tao<sup>2</sup>, D Stefan<sup>3</sup>, W Kun<sup>\*,1</sup> and L Pei-Feng<sup>\*,1</sup>

Autophagy is required for the maintenance of cardiomyocytes homeostasis. However, the abnormal autophagy could lead to the development of heart failure. Autophagy is enhanced during myocardial ischemia/reperfusion; it remains to elucidate the molecular regulation of autophagy. We report here that miR-325, ARC and E2F1 constitute an axis that regulates autophagy. Our results showed that miR-325 expression is upregulated upon anoxia/reoxygenation and ischemia/reperfusion. Cardiomyocyte-specific overexpression of the miR-325 potentiates autophagic responses and myocardial infarct sizes, whereas knockdown of miR-325 inhibited autophagy and cell death. We searched for the downstream mediator of miR-325 and identified that ARC is a target of miR-325. ARC transgenic mice could attenuate autophagy and myocardial infarction sizes upon pressure-overload-induced heart failure, whereas ARC null mice exhibited an increased autophagic accumulation in the heart. The suppression of ARC by miR-325 led to its inability to repress autophagic program. In exploring the molecular mechanism by which miR-325 expression is regulated, our results revealed that the transcription factor E2F1 contributed to promote miR-325 expression. E2F1 null mice demonstrated reduced autophagy and myocardial infarction sizes upon ischemia/reperfusion. Our present study reveals a novel autophagic regulating model that is composed of E2F1, miR-325 and ARC. Modulation of their levels may provide a new approach for tackling cardiac failure.

*Cell Death and Differentiation* (2014) 21, 967–977; doi:10.1038/cdd.2014.18; published online 14 February 2014

Autophagy is a process of catabolism of cellular components including protein aggregates, organelles and viruses, and is necessary for the maintenance of cell homeostasis.<sup>1–4</sup> The morphological character of autophagy is the formation of autophagosome that encompasses cellular components and subsequently fuses with lysosomes. It finally degrades the inclusion into reusable amino acids and other materials.<sup>5,6</sup> However, the abnormal autophagy is related to a variety of pathological disorders including cancer, neurodegenerative and cardiovascular diseases.<sup>7–10</sup>

MicroRNAs (miRNAs) are about 22-nucleotides long and act as negative regulators of gene expression.<sup>11–14</sup> Strikingly, a single microRNA is even able to modulate complex physiological or disease phenotypes by regulating the entire functional networks.<sup>12,15,16</sup> They can bind to the 3' untranslated region (3'UTR) of mRNAs, thereby inhibiting mRNA translation or promoting mRNA degradation.<sup>11</sup> They participate in the regulation of a variety of cellular events such as apoptosis, proliferation, development, differentiation and cell conversion. For example, miR-200c strongly suppresses the ability of normal mammary stem cells to form mammary ducts and tumor formation.<sup>17</sup> miR-31 uses multiple mechanisms to oppose the breast cancer metastasis.<sup>18</sup> miR-208 regulates cardiac growth and gene expression in response to stress and hormonal signaling.<sup>14</sup>

Autophagy is regulated by a variety of factors in which the autophagy-related genes (ATGs) control the different stages of autophagy including initiation and elongation.<sup>1,19</sup> Beclin 1 is ATG6 and is required for the formation of the autophagosome in autophagy.<sup>20</sup> LC3-I is ATG8, which is conjugated to the lipid phosphatidylethanolamine to form LC3-II that fuses with the inner and outer surfaces of the autophagosome.<sup>21</sup> Intriguingly, apoptosis and autophagy have a cross-talk, and some proteins can regulate both autophagy and apoptosis. ATG12–ATG3 forms a complex that produces an expansion in mitochondrial mass and inhibits cell death mediated by mitochondrial pathways.<sup>22</sup> Bcl-2 can inhibit apoptosis and autophagy.<sup>7,23</sup> Calpain-mediated cleavage of Atg5 switches autophagy to apoptosis.<sup>24</sup> Inhibition of autophagy leads to the occurrence of apoptosis.<sup>25</sup>

A few reports have shown that miRNAs are involved in the regulation of autophagy. miR-101 is a potent inhibitor of autophagy.<sup>26</sup> miR-30a sensitizes tumor cells to *cis*-platinum via suppressing Beclin 1-mediated autophagy.<sup>27</sup> miR-204 regulates autophagy through LC3-II.<sup>28</sup> It remains largely unknown as to how autophagy is regulated by miRNAs.

Apoptosis repressor with caspase recruit domain (ARC) is a protein not only highly expressed in the heart and skeletal muscle<sup>29,30</sup> but also in a variety of cancers.<sup>31,32</sup> It was originally identified to be a caspase-inhibiting protein and can inhibit apoptosis induced by a variety of stimuli.<sup>30</sup> Further

<sup>1</sup>Division of Cardiovascular Research, State Key Laboratory of Biomembrane and Membrane Biotechnology, Institute of Zoology, Chinese Academy of Sciences, Beijing 100101, China; <sup>2</sup>FU WAI Hospital CAMS&PUMC, National Center for Cardiovascular Diseases, Beijing 10037, China and <sup>3</sup>Franz-Volhard-Clinic, Humboldt University of Berlin, Berlin 13125, Germany

\*Corresponding author: L Pei-Feng or W Kun, Institute of Zoology, Chinese Academy of Sciences, State Key Laboratory of Biomembrane and Membrane Biotechnology, 1 Beichen West Road, Chaoyang District, Beijing 100101, China. Tel/Fax: +86 10 64807176; E-mail: lpeifeng@ioz.ac.cn (LP-F) or Tel/Fax: +86 10 64807158; E-mail: wangk696@ioz.ac.cn (WK)

<sup>4</sup>These authors contributed equally to this work.

**Keywords:** miR-325; ARC; autophagy

**Abbreviations:** miRNAs, microRNAs; ARC, apoptosis repressor with caspase recruitment domain; A/R, anoxia/reoxygenation; I/R, ischemia/reperfusion; LC3, microtubule-associated protein 1 light chain 3; BFA, Bafilomycin A1; 3-MA, 3-methyladenine; qRT-PCR, quantitative reverse transcription polymerase chain reaction; C-Casp3, cleaved caspase-3; TP, target protector

Received 23.9.13; revised 31.12.13; accepted 14.1.14; Edited by D Rubinsztein; published online 14.2.14

evidence demonstrates that it also can bind to Bax<sup>33</sup> and Puma,<sup>29</sup> thereby quenching their apoptotic signal. It is not yet clear whether ARC can regulate autophagic program.

Our present study unveils that ARC is an antiautophagic protein. ARC knockout mice exhibit accelerated autophagy, whereas ARC transgenic mice can attenuate autophagy. In searching for the mechanism by which ARC is down-regulated under autophagic condition, we identified miR-325 participates in the suppressing of ARC translation. miR-325 initiates autophagic program through targeting ARC. We further found that E2F1 can promote the expression of miR-325. miR-325 is a downstream mediator of E2F1 in autophagic cascades. Taken together, our findings provide novel evidence that miRNA can regulate autophagic program.

## Results

**ARC regulates autophagy under the physiological condition.** To understand the role of ARC in the machinery of autophagy, we employed ARC knockout mice. A characteristic of autophagy is the recruitment of the microtubule-associated protein 1 light chain 3 (LC3) to autophagic vesicles. Evidence for the increased autophagic activity was revealed by an augmentation in LC3-II levels in an ARC-deficient heart compared with wild-type mice. Noticeably, LC3 processing was not obviously detected in other tissues where ARC is not abundantly expressed (Figure 1a). These

data indicate that ARC-deficient mice exhibited an autophagic response specific to the heart and not reflective of other global responses. The electron micrographic (EM) analysis of ventricular tissue was also used to identify double-membrane bound autophagic vesicles. ARC-deficient hearts demonstrated extensive vacuolization (Figure 1b). Taken together, these data indicate an increased autophagic accumulation upon ARC deficiency.

### ARC inhibits autophagy under the pathological condition.

We attempted to understand the role of ARC in autophagy under the pathological condition and observed that anoxia/reoxygenation (A/R) could reduce the level of ARC (Supplementary Figure 1A). During autophagy, LC3-II relocates to the autophagosomal membranes. Thus, the accumulation of GFP-LC3 puncta provides an effective way to detect autophagosomes. We found that A/R resulted in an increased GFP-LC3 punctate structures (Supplementary Figure 1B). Enforced expression of ARC significantly reduced punctate accumulations of GFP-LC3 (Figure 2a) and LC3-II levels (Supplementary Figure 2A). To determine whether ARC can inhibit the formation of autophagosomes or promote the degradation, we measured p62 and observed that enforced expression of ARC caused an increase in p62 levels (Supplementary Figure 2B). Autophagic flux is considered to be a better indicator of autophagic activation. We measured the autophagic flux in the presence and absence of lysosomal

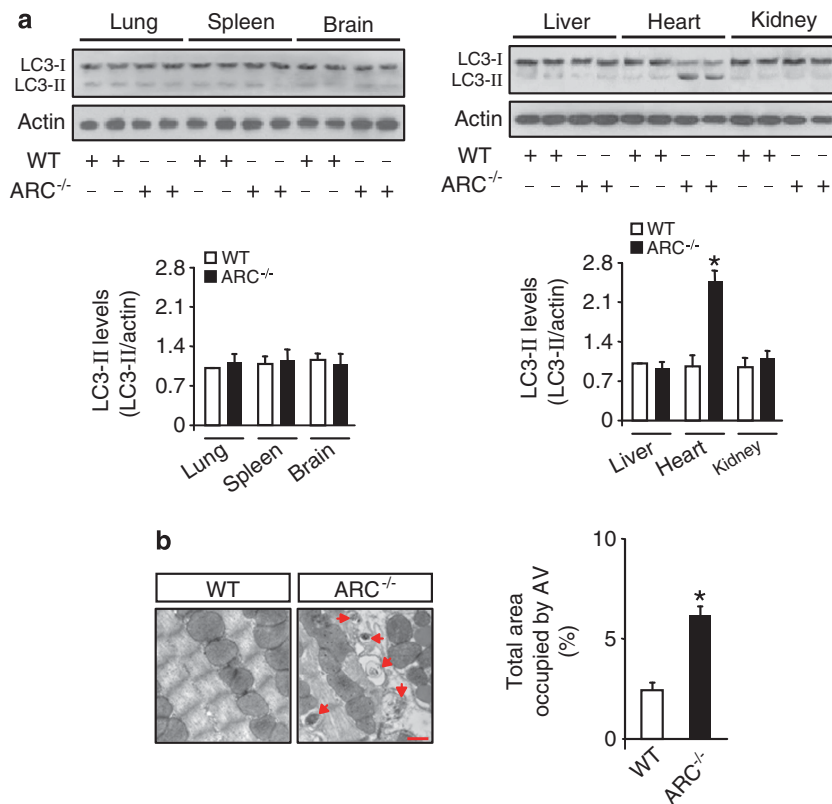


**Figure 1** ARC regulates autophagy under the physiological condition. (a) Representative immunoblot for conversion of LC3-I to LC3-II in the organ of the lung, spleen, brain, liver, heart and kidney from ARC-deficient mice or WT mice. The positions of LC3-I and LC3-II are indicated. The densitometric analysis of western blot of LC3-II is shown (lower panel). \* $P < 0.05$ , versus WT. (b) Representative electron micrographs (EM) of hearts from ARC-deficient mice and WT mice show the presence of autophagosomes (arrow). Bar = 500 nm. Quantification of autophagic vacuoles is shown in the right panel. \* $P < 0.05$

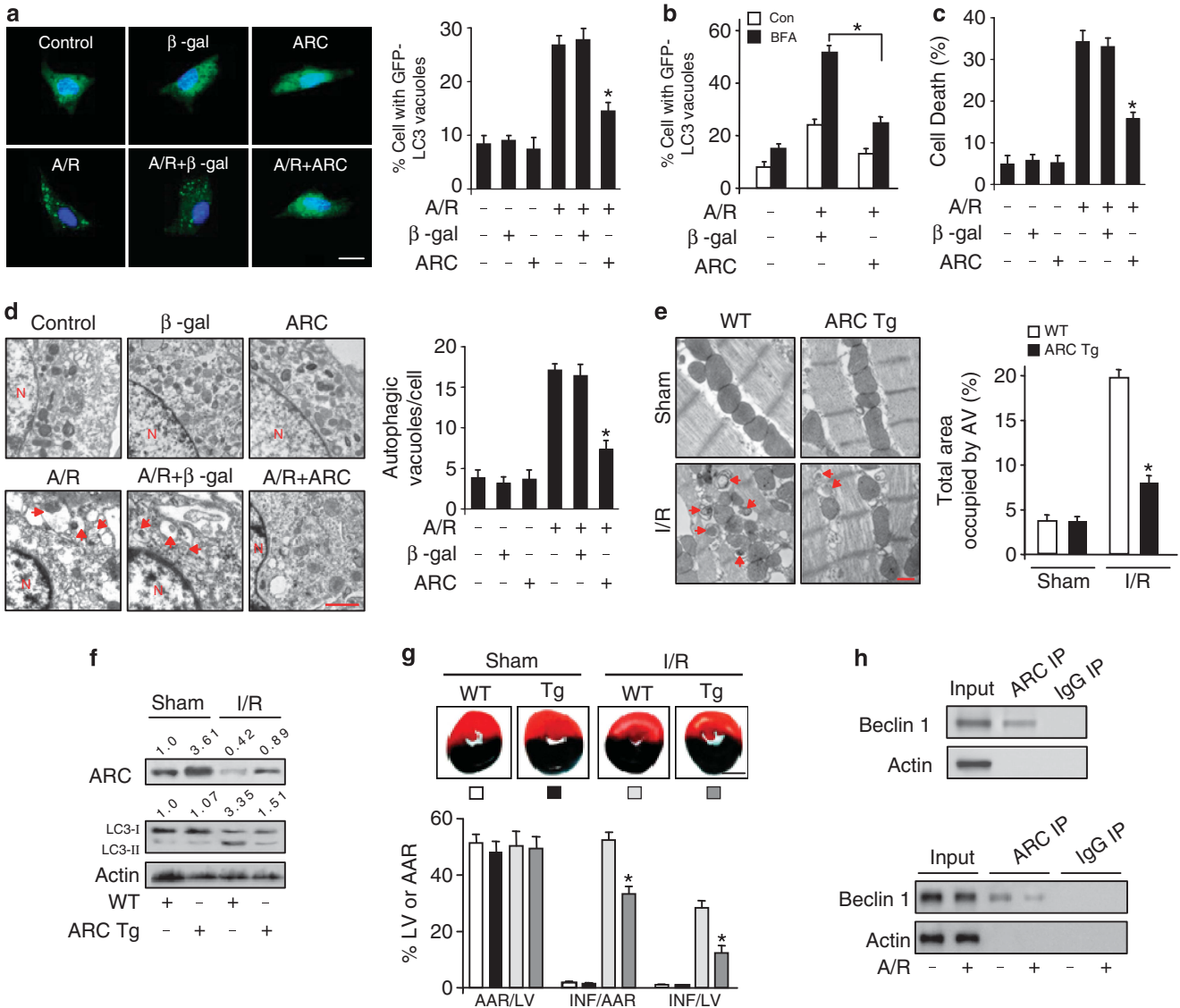


**Figure 2** ARC inhibits autophagy under the pathological condition. (a) ARC inhibits punctate accumulations of GFP-LC3 induced by A/R. Cardiomyocytes were infected with adenoviral GFP-LC3, ARC and  $\beta$ -gal, and then exposed to A/R. Representative photos of GFP-LC3 cells were shown in left panel, and the percentage of cells with GFP-LC3 puncta was quantified in right panel.  $*P < 0.05$  versus A/R alone. Bar = 20  $\mu$ m. (b) Autophagic flux assay. Cardiomyocytes were infected with adenoviral ARC (80 moi) and  $\beta$ -gal, and then exposed A/R. Twenty-four hours after infection, cells were untreated or treated with bafilomycin A1 (BFA, 100 nM) for 1 h. The percentage of cells with GFP-LC3 puncta was quantified.  $*P < 0.05$ . (c, d) ARC reduces cell death and autophagic vacuoles. Cardiomyocytes were infected with adenoviral ARC or  $\beta$ -gal and then exposed to A/R. Quantitation of cell death was shown in (c). Representative EM images and quantification of autophagic vacuoles were shown in (d). Bar = 500 nm. The arrows depict autophagosomes, and the nucleus is denoted by N.  $*P < 0.05$  versus A/R alone. (e, f) Autophagy was reduced in ARC transgenic mice upon I/R. ARC transgenic mice (Tg) or wild-type mice (WT) were subjected to 45 min ischemia and 3 h reperfusion (I/R). The representative electron micrographs of hearts were shown (e). ARC and LC3 levels were analyzed by immunoblot (f). The densitometric analysis of western blot of ARC and LC3-II is shown. (g) ARC transgenic mice exhibit reduced myocardial infarction upon I/R. ARC transgenic mice (ARC Tg) and wild-type mice (WT) were exposed to I/R. The upper panels are representative photos of midventricular myocardial slices. The lower panel shows infarct sizes. Area-at-risk (AAR), left ventricle (LV), infarct area (INF).  $n = 6$ ,  $*P < 0.05$  versus WT + I/R. Bar = 2 mm. (h) ARC interacts with Beclin 1. Immunoprecipitation was performed using an ARC antibody in cardiomyocytes in the presence or absence of A/R. The anti-IgG served as a control. Beclin 1 levels were analyzed by immunoblot

inhibitor bafilomycin A1 (BFA), which inhibits fusion of autophagosome and lysosome. Our results showed that ARC reduced autophagosome abundance even in the presence of BFA (Figure 2b). In addition, enforced expression of ARC significantly reduced cell death induced by A/R (Figure 2c). The results in EM analysis show that ARC reduced autophagic vesicles in cardiomyocytes (Figure 2d). Taken together, these results suggest that ARC inhibits

autophagy and cell death induced by A/R in cardiomyocytes. We tested whether ARC has a role in the pathogenesis of myocardial infarction. ARC transgenic mice could attenuate autophagy (Figures 2e and f) and myocardial infarction sizes (Figure 2g), as well as ameliorated myocardial function (Supplementary Figure 2C), in response to ischemia/reperfusion (I/R). These data suggest that ARC is able to inhibit autophagy and autophagic cell death in the heart.

We investigated the mechanism by which ARC regulates autophagy. Beclin 1 is a well-known key regulator of autophagy,<sup>34,35</sup> and recent studies have shown that Beclin 1 mediates the autophagic cell death in cardiomyocytes.<sup>36</sup> Our results also showed that knockdown of Beclin 1 attenuated autophagy (Supplementary Figure 3A) and cell death (Supplementary Figure 3B). Overexpression of Beclin 1 sensitized cells to undergo death, and increased cell death was observed upon both A/R and Beclin 1 treatment in the presence of a lysosomal inhibitor bafilomycin A1 (Supplementary Figure 3C). These lines of evidence encouraged us to test whether there is a cross-talk between ARC and Beclin 1. We performed immunoprecipitation. The results showed that Beclin 1 was immunoprecipitated with an anti-ARC antibody, and the immunoprecipitated amount was decreased upon A/R condition (Figure 2h). Thus, it appears that Beclin 1 is a target of ARC in the cascade of autophagy. Knockdown of ATG5 also attenuated cell death induced by A/R (Supplementary Figure 3D) and Beclin 1 treatment (Supplementary Figure 3E), but ATG5 failed to co-immunoprecipitate with ARC (data not shown). It is reported that Bcl-2 could bind to Beclin 1 and inhibit Beclin 1-dependent autophagy.<sup>7</sup> Thus, we explore whether ARC can affect Beclin 1 binding to Bcl-2. Our results showed that overexpression (Supplementary Figure 3F, upper panel) or knockdown (Supplementary Figure 3F, lower panel) of ARC doesn't affect the levels of Bcl-2-immunoprecipitated Beclin 1.

To further test whether ARC can regulate autophagic cell death, we compared the effect of z-VAD-fmk (a pancaspase inhibitor) and ARC on autophagic cell death. Overexpression of Beclin 1 sensitized cells to undergo death, and ARC could inhibit this cell death. ARC effect is much more than that of z-VAD-fmk (Supplementary Figures 4A and B). Whereas, the caspase-3 activity were partly inhibited by ARC compared with z-VAD-fmk (Supplementary Figure 4C). In cardiomyocytes, we compared the effect of z-VAD-fmk alone, the autophagy inhibitor 3-methyladenine (3-MA) alone and their combination on cell death upon A/R. The inhibitory effect of ARC on cell death was more effective than z-VAD-fmk alone, 3-MA alone or their combination (Supplementary Figure 4D). In the animal model, we compared the effect of z-VAD-fmk alone, Beclin 1 siRNA alone and their combination with ARC transgenic mice on myocardial infarction. ARC transgenic mice exhibited a significant reduction in myocardial infarction size than the mice treated with z-VAD-fmk alone, Beclin 1 siRNA alone or their combination (Supplementary Figure 4E), suggesting that the

effect of ARC is not solely on apoptosis and ARC can also regulate autophagic cell death. Taken together, these data suggest that the ARC can regulate autophagy *in vitro* and *in vivo*.

**ARC is a target of miR-325.** miRNA is able to suppress gene expression. To explore the underlying mechanism responsible for ARC downregulation, we tested whether miRNA participates in the regulation of ARC expression. miR-325 is expressed at a low level in the heart but was upregulated upon A/R (Supplementary Figure 5A) and I/R (Supplementary Figure 5B). We analyzed its potential targets using the online software of RNAhybrid and found that ARC is a potential target of miR-325 in mouse (Figure 3a), human and rat (Supplementary Figure 5C). We tested whether miR-325 is related to ARC expression. Enforced expression of miR-325 could reduce ARC levels (Figure 3b). Knockdown of miR-325 increased the ARC levels upon A/R (Figure 3c). Thus, it appears that miR-325 is a regulator of ARC. To understand whether miR-325 can directly target ARC, we prepared the luciferase constructs (Figure 3d). The luciferase assay revealed that miR-325 could suppress the translational activity of ARC (Figure 3e). The administration of miR-325 antagomir but not the antagomir negative control (antagomir-NC) could block the effect of miR-325. Introduction of mutations that disrupt base pairing between miR-325 and ARC rescued luciferase expression (Figure 3f) and ARC protein expression (Figure 3g). We also employed the target protector technology in which a target protector is able to disrupt the specific interaction of miRNA–mRNA pairs. We observed that the inhibitory effect of miR-325 on ARC was reduced in the presence of ARC target protector (Figure 3h). Furthermore, different lines (Figure 3i) of miR-325 transgenic mice (Supplementary Figure 6) demonstrated reduced levels of ARC in the animal model (Figure 3j). These data suggest that the inhibitory effect of miR-325 on ARC translation is specific.

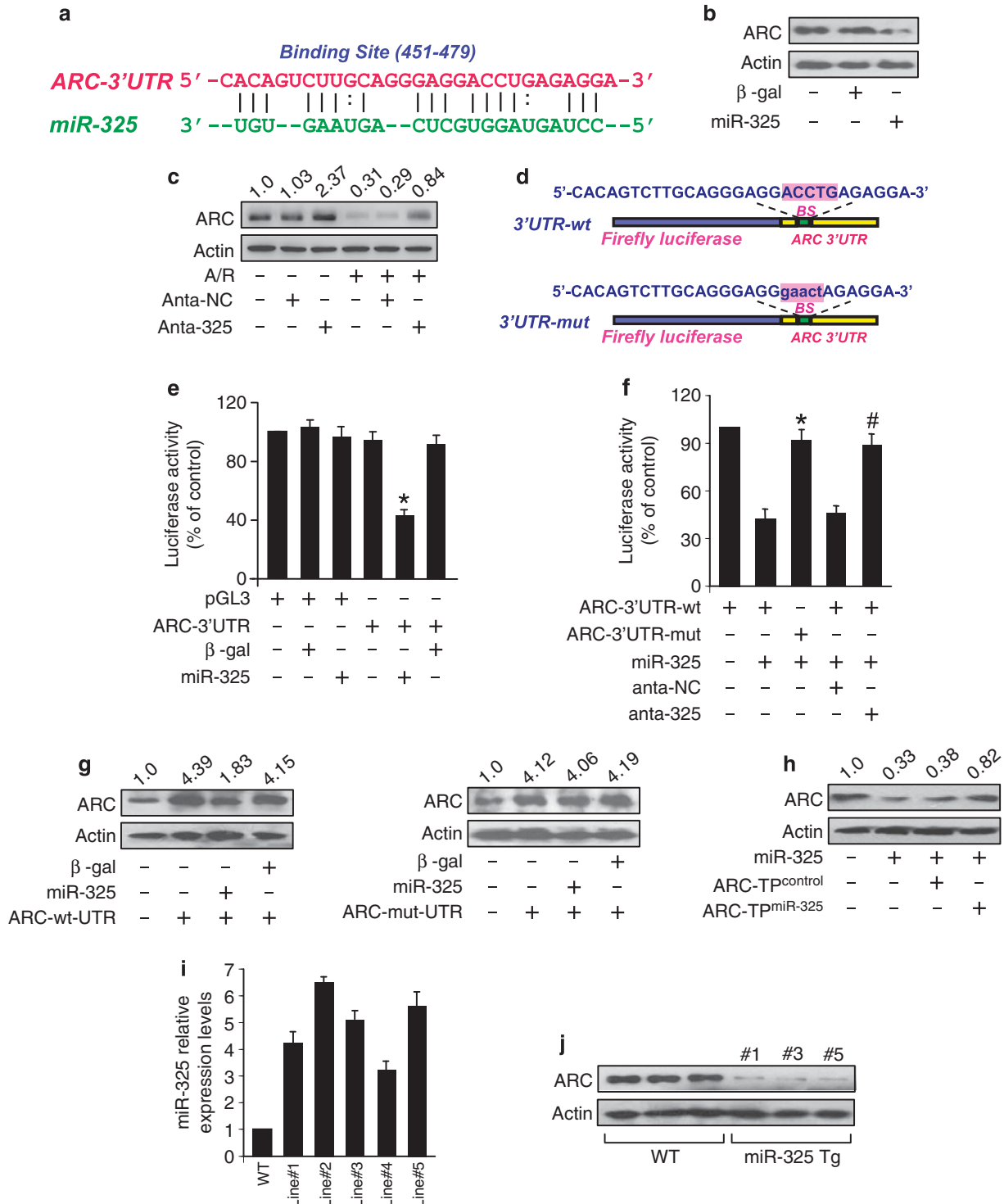
**miR-325 conveys the autophagic signal.** We tested whether miR-325 has a functional role. In the cellular model, knockdown of miR-325 (Supplementary Figure 7A) reduced punctate accumulations of GFP-LC3 (Figure 4a) and induced an increase in p62 levels (Supplementary Figure 7B) upon A/R. Further, we measured the autophagic flux in the presence and absence of bafilomycin A1. The results showed that knockdown of miR-325 reduced autophagosome abundance even in the presence of BFA (Figure 4b). In addition, knockdown of miR-325 reduced cell death induced by A/R

**Figure 3** ARC is a target of miR-325. (a) The miR-325 targeting site in ARC 3'UTR was shown. (b) miR-325 suppresses ARC expression. Cardiomyocytes were infected with adenoviral miR-325 or the  $\beta$ -gal. ARC expression was analyzed by immunoblot 48 h after infection. (c) Knockdown of miR-325 attenuates the decrease in ARC levels upon A/R. Cardiomyocytes were transfected with miR-325 antagomir (anta-325) or antagomir negative control (anta-NC), and then treated with A/R. Cells were collected 4 h after treatment for the analysis of ARC by immunoblot. The densitometric analysis of western blot of ARC is shown. (d–f) miR-325 suppresses ARC translation. d: wild type (wt) and a mutated (mut) ARC-3'UTR in the miR-325-binding sites were shown. e: HEK293 cells were infected with adenoviral miR-325 or  $\beta$ -gal, and then transfected with the luciferase constructs of ARC-3'UTR or the empty vector pGL3, \* $P < 0.05$  versus ARC-3'UTR alone. f: HEK293 cells were infected with adenoviral miR-325, transfected with miR-325 antagomir (anta-325) or the antagomir negative control (anta-NC), the luciferase constructs of the wild-type ARC-3'UTR (ARC-3'UTR-wt) or the mutated ARC-3'UTR (ARC-3'UTR-mut). \* $P < 0.05$  versus ARC-3'UTR-wt plus miR-325. # $P < 0.05$  versus ARC-3'UTR-wt plus miR-325 plus anta-NC. (g) miR-325 can suppress the expression of ARC with wild type but not mutated 3'UTR. Cardiomyocytes were co-infected with the adenoviral miR-325 or  $\beta$ -gal, along with ARC with wild-type 3'UTR (ARC-wt-UTR) or the mutated UTR (ARC-mut-UTR). ARC levels were detected by immunoblot. The densitometric analysis of western blot of ARC is shown. (h) ARC target protector reduces the inhibitory effect of miR-325 on ARC expression. Cardiomyocytes were infected with adenoviral miR-325, transfected with the target protector (ARC-TP<sup>miR-325</sup>) or the control (ARC-TP<sup>control</sup>). ARC was analyzed by immunoblot. The densitometric analysis of western blot of ARC is shown. (i) The expression of miR-325 was analyzed by qRT-PCR from wild type and miR-325 transgenic mice of different lines. The results were normalized to U6. (j) miR-325 suppresses the expression of ARC in the animal model. ARC expression was analyzed by immunoblot from WT and miR-325 transgenic mice of lines 1, 3 and 5

(Figure 4c) and autophagic vesicles in cardiomyocytes observed by EM analysis (Figure 4d). In the animal model, miR-325 transgenic mice potentiate autophagic responses revealed by EM analysis of ventricular tissue (Figure 4e), an increase in LC3-II levels (Figure 4f), an enlarged myocardial infarct sizes (Figure 4g) and pronounced cardiac dysfunction (Supplementary Figure 7C). These data suggest that

miR-325 participates in mediating the signal for autophagy and cell death in the heart.

**miR-325 exerts its autophagic effect through ARC.** We explored how miR-325 exerts its effect on autophagy. The inhibitory effect of miR-325 on ARC expression encouraged us to test whether ARC is a mediator of miR-325. Although



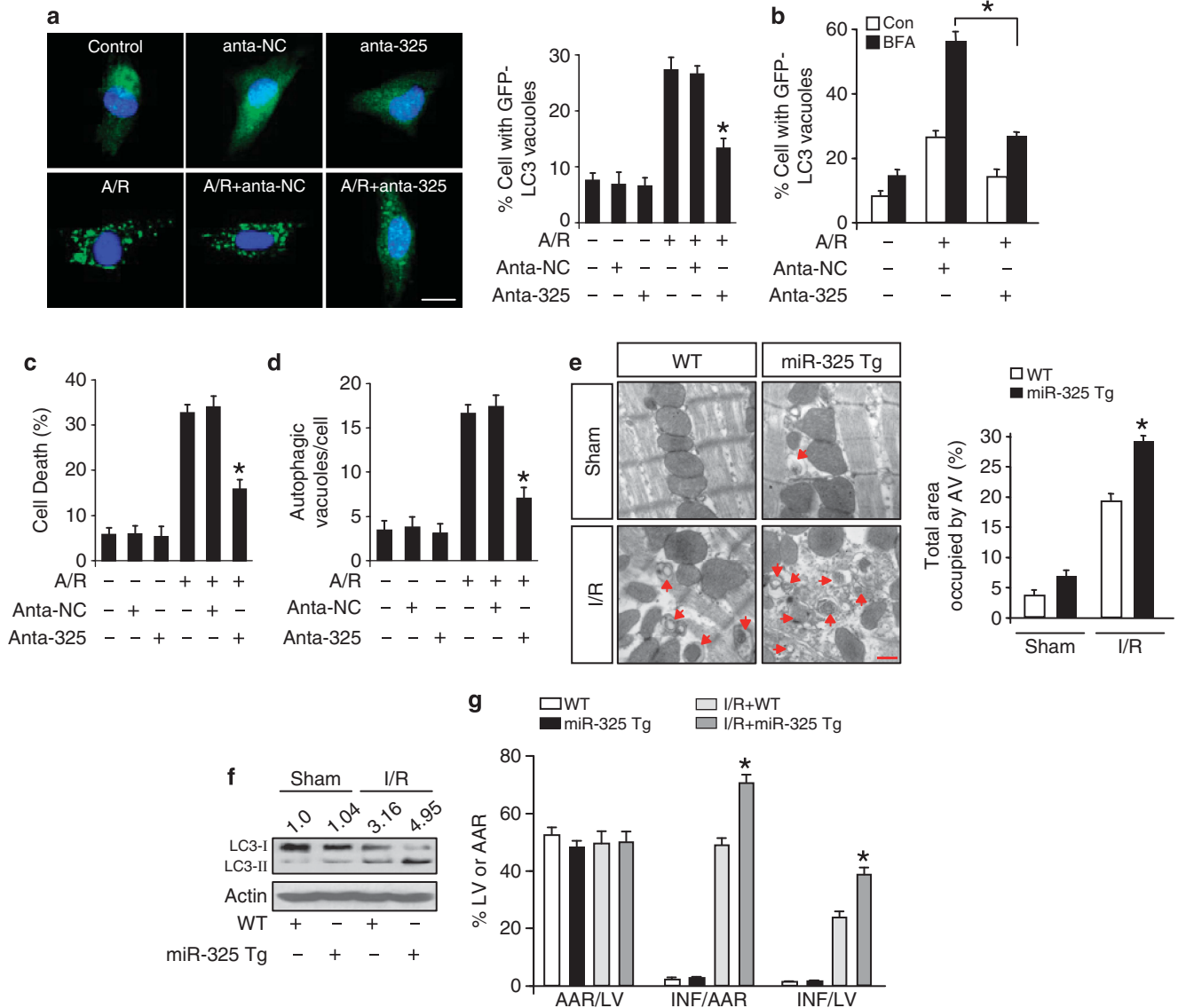


**Figure 4** miR-325 conveys the autophagic signal. (a) Knockdown of miR-325 inhibits punctate accumulations of GFP-LC3. Cardiomyocytes were infected with adenoviral GFP-LC3 and transfected with antagomir-325 (anta-325) or antagomir-NC (anta-NC). Twenty-four hours after transfection cells were treated with A/R. Representative images show GFP-LC3 staining (left panel), bar = 20  $\mu$ m. The percentage of cells with GFP-LC3 puncta was quantified in right panel. \* $P < 0.05$  versus A/R alone. (b) Autophagic flux assay. Cardiomyocytes were infected with adenoviral GFP-LC3 and transfected with antagomir-325 (anta-325) or antagomir-NC (anta-NC), and then exposed A/R. Twenty-four hours after transfection, cells were untreated or treated with bafilomycin A1 (BFA, 100 nM) for 1 h. The percentage of cells with GFP-LC3 puncta was quantified. \* $P < 0.05$ . (c, d) Knockdown of miR-325 reduces cell death and autophagic vacuoles. Cardiomyocytes were treated as described in (a). Quantitation of cell death was shown in (c). Quantitation of autophagic vacuoles was shown in (d). \* $P < 0.05$  versus A/R alone. (e, f) Autophagy is augmented in miR-325 transgenic mice upon I/R. miR-325 transgenic mice (miR-325 Tg) or wild-type mice (WT) were subjected to 45 min ischemia and 3 h reperfusion (I/R). Representative electron micrographs of hearts are shown (e). ARC and LC3 levels were analyzed by immunoblot (f). The densitometric analysis of western blot of ARC and LC3-II are shown. (g) miR-325 transgenic mice show more severe myocardial infarction. miR-325 transgenic mice (Tg) and wild-type mice (WT) were exposed to I/R. The infarct sizes were shown.  $n = 6$ , \* $P < 0.05$  versus WT + I/R

knockdown of miR-325 could inhibit autophagy and cell death, this effect was significantly abolished by knockdown of endogenous ARC (Figures 5a and b). To confirm the relationship between miR-325 and ARC in autophagy machinery, we employed the target protector technology. To this end, we produced ARC target protector and observed that autophagy and cell death was reduced in the presence of ARC target protector (Figures 5c and d). These data suggest that miR-325 targets ARC in the cascades of autophagy and cell death.

To better understand the relationship between miR-325 and ARC, we tested whether these two factors have an impact on the animal model. We produced miR-325 transgenic mice, miR-325/ARC-with UTR bitransgenic mice (325/ARC-UTR) and miR-325/ARC-without UTR bitransgenic mice (325/ARC) (Figure 5e). The 325/ARC but not 325/ARC-UTR bitransgenic mice exhibited a reduced autophagic response (Figure 5f) and myocardial infarct sizes (Figure 5g). Thus, ARC and miR-325 have a cross-talk in the animal model.

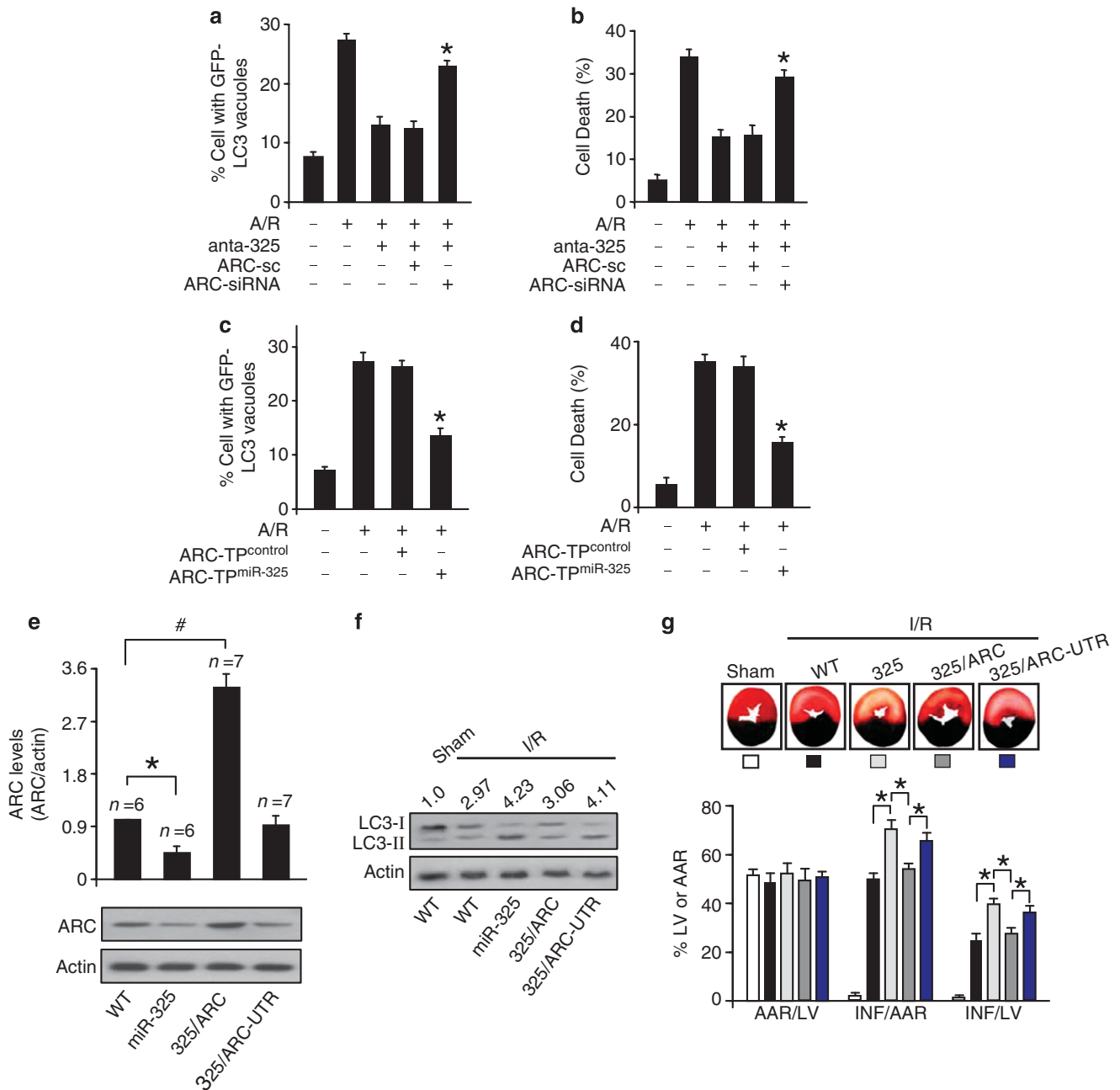


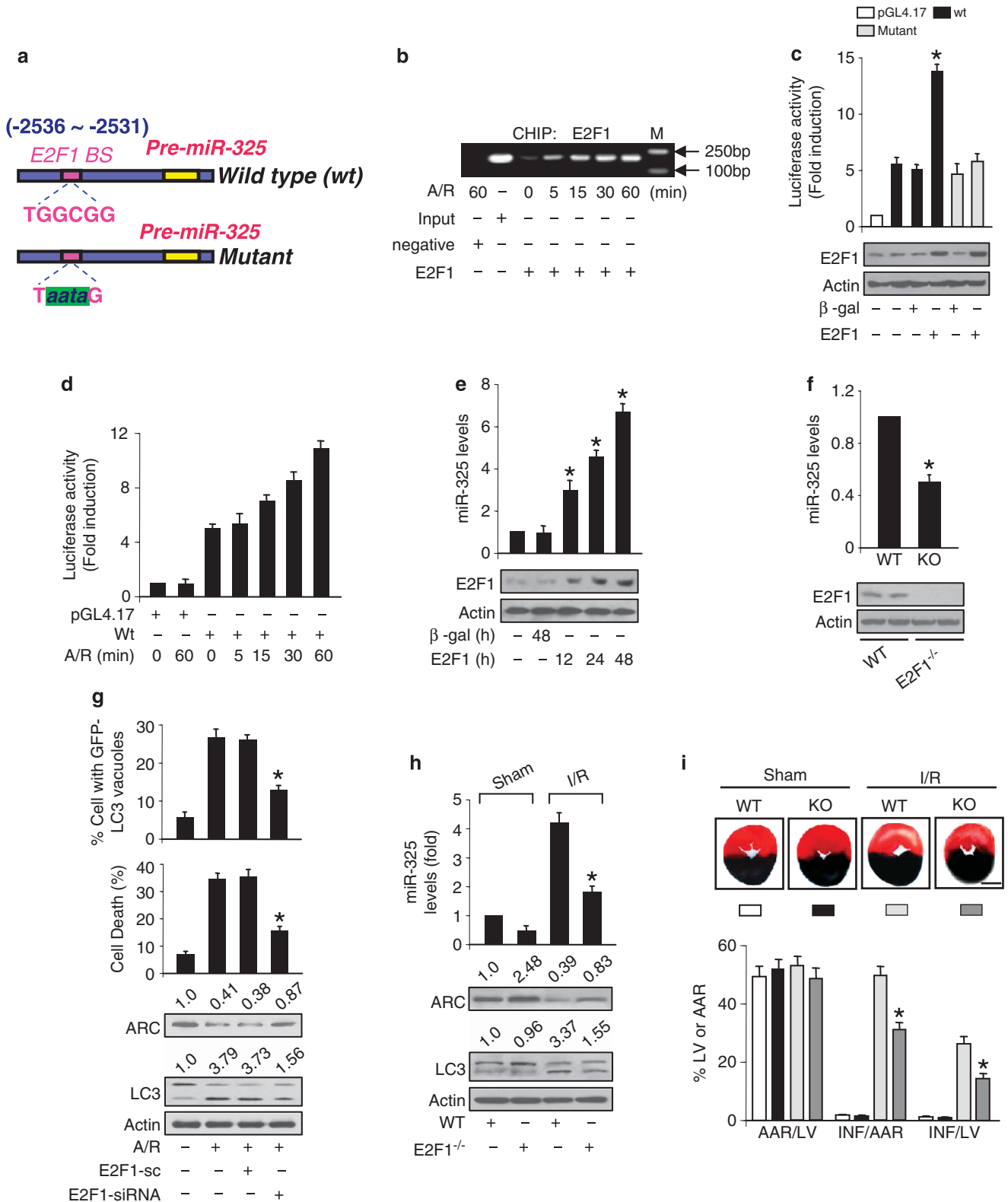
**Figure 5** miR-325 exerts its autophagic effect through ARC. (a, b) ARC and miR-325 have a cross-talk in autophagy and cell death. Cardiomyocytes were infected with adenoviral GFP-LC3 and ARC-siRNA or its scramble form (ARC-sc), transfected with miR-325 antagomir (anta-325) or antagomir negative control (anta-NC), and then treated with A/R. Quantitation of GFP-LC3 staining (a) and cell death (b) are shown. \* $P < 0.05$  versus A/R plus anta-325. (c, d) ARC Target Protector attenuates autophagy and cell death. Cardiomyocytes were infected with adenoviral GFP-LC3, transfected with the target protector (ARC-TP<sup>miR-325</sup>) or the control (ARC-TP<sup>control</sup>), and then exposed to A/R. Quantitation of GFP-LC3 staining (c) and cell death (d) are shown. \* $P < 0.05$  versus A/R alone. (e) ARC levels analyzed by immunoblot in wild-type mice (WT), miR-325 transgenic mice (325), miR-325/ARC bitransgenic mice (325/ARC) and miR-325/ARC-3'UTR bitransgenic mice (325/ARC-UTR). Quantitative analysis of ARC levels is shown in upper panel. \*\* $P < 0.05$ . (f) miR-325/ARC bitransgenic mice exhibit reduced autophagy. WT, miR-325 transgenic mice, miR-325/ARC bitransgenic mice and miR-325/ARC-UTR bitransgenic mice were exposed to I/R. LC3 levels were analyzed by immunoblot. The densitometric analysis of western blot of LC3-II is shown. (g) miR-325/ARC bitransgenic mice exhibit reduced myocardial infarction. Wild type (WT), miR-325 (325) transgenic mice, miR-325/ARC (325/ARC) bitransgenic mice and miR-325/ARC-3'UTR (325/ARC-UTR) bitransgenic mice were exposed to I/R. The upper panels are representative photos of midventricular myocardial slices. The lower panel shows infarct sizes.  $n = 6$ , \* $P < 0.05$ . Bar = 2 mm

**E2F1 regulates miR-325 expression.** We asked how miR-325 expression is regulated under the pathological condition. To address this question, we analyzed the promoter region of mouse miR-325 and observed that there is an optimal

consensus binding site of E2F1 (Figure 6a). In addition, there are binding sites in the promoter regions of human and rat miR-325 (Supplementary Figure 8A). We tested whether E2F1 can bind to the promoter region of miR-325. The ChIP

assay revealed that E2F1 bound to the miR-325 promoter under the physiological condition. A/R treatment led to an increase in the association levels of E2F1 with miR-325 promoter (Figure 6b). The luciferase assay demonstrated

that E2F1 could stimulate the activity of miR-325 wild-type promoter but not that of the mutant (Figure 6c). A/R induced an elevation in E2F1 expression levels (Supplementary Figure 8B) and miR-325 promoter activity (Figure 6d).





Enforced expression of E2F1 led to an elevation of miR-325 levels (Figure 6e). Knockdown of E2F1 induced a decrease in miR-325 expression levels (Supplementary Figure 8C). E2F1 knockout mice exhibited a low level of miR-325 (Figure 6f). These data suggest that E2F1 can transcriptionally upregulate miR-325.

We investigated the role of E2F1 in autophagy in cardiomyocytes and myocardial infarction. Knockdown of E2F1 was able to attenuate autophagy and cell death upon A/R (Figure 6g, Supplementary Figure 8D). Enforced expression of E2F1 led to autophagy and cell death (Supplementary Figures 8E and F). E2F1 knockout mice demonstrated reduced autophagy revealed by LC3-II levels (Figure 6h) and myocardial infarction sizes (Figure 6i) upon ischemia/reperfusion. These data suggest that E2F1 participates in mediating the signal for autophagy and cell death in the heart.

## Discussion

Our present study revealed that miR-325 is integrated into the autophagic machinery. Further, we identified ARC was able to regulate the autophagic program. miR-325 provokes autophagy through repressing ARC. Our results demonstrate that miR-325 and ARC constitute an axis controlling autophagy and cell death, and target that this axis can bring beneficial effect.

Autophagy is a physiological and evolutionarily conserved phenomenon maintaining homeostatic functions like protein degradation and organelle turnover. Autophagy can have a cytoprotective role in cells under conditions of nutrient starvation.<sup>25</sup> Yet accumulating data show that the autophagic machinery can also be recruited to kill cells under certain conditions generating a caspase-independent form of programmed cell death, named autophagic cell death. The abnormal autophagy is related to a variety of pathological disorders including cancer, neurodegenerative and cardiovascular diseases,<sup>7–10</sup> and the autophagic machinery may also be used for cell self-destruction.<sup>37</sup> Consistent with these reports, our results suggested that inhibition of autophagy protects cell death induced by the myocardial I/R injury. Further investigation on how excessive autophagy affects cell

signaling and growth under pathological condition will provide more targets to understand the basis of the diseases.

ARC has an important role in regulating the apoptotic pathway and inhibits apoptosis through different manners. It can interact with Fas, FADD and Bax,<sup>33,38</sup> inhibit cytochrome c release<sup>39</sup> and maintain mitochondrial membrane potential.<sup>40,41</sup> These lines of evidence suggest that ARC is a critical factor for maintaining the cellular function. Our present work reveals that ARC participates in the regulation of autophagy to maintain the equilibrium between autophagic cell death and cell survival. In particular, we found that ARC-deficient mice exhibit more autophagy, suggesting that ARC is a physiological regulator of autophagy. Starvation is a physiologic inducer of autophagy, future studies can test whether ARC is able to influence autophagic program of starvation.

Other antiapoptotic proteins can regulate autophagic program. For example, Bcl-2 binds to Beclin 1 and disrupts its autophagy function. In the absence of Bcl-2 binding, Beclin 1 mutants induce excessive autophagy and promote cell death.<sup>7</sup> Bcl-xL can interact with ATG5 thereby preventing cytochrome c release and caspase activation.<sup>24</sup> There is a complex relationship between apoptosis and autophagy. Our present work shows that ARC can bind to Beclin 1 and may disrupt its autophagy function. The direct interaction of ARC with Beclin 1 is of particular interest with respect to the heart, because cardiomyocytes have the limited proliferative capability, and induction of autophagic cell death in cardiomyocytes may lead to pathophysiological disorders such as myocardial infarction and heart failure. ARC is highly expressed in cardiomyocytes. The ability of ARC to directly associate with Beclin 1 enables ARC to more efficiently control autophagic cell death so that the heart does not lose more cardiomyocytes under the physiological as well as pathological conditions. Our results may have important therapeutic implications for the employment of ARC in the treatment of autophagy-related diseases.

Growing evidence has shown that miRNA can regulate apoptosis. For example, miR-23a-27a-24-2 cluster induces caspase-dependent and -independent apoptosis.<sup>42</sup> miR-101 and miR-29b repress the antiapoptotic protein Mcl-1.<sup>43</sup> Also, other reports show that miRNAs can regulate the autophagy. For example, reduced levels of miR-23b increase levels of

**Figure 6** E2F1 regulates autophagy through miR-325 and ARC. (a) Mouse miR-325 promoter region contains a potential E2F1 binding site. The promoter of miR-325 was synthesized and linked to luciferase reporter gene. The mutations were introduced to the binding site. (b) E2F1 binds to the promoter of miR-325. ChIP assay was performed using cardiomyocytes treated with A/R at the indicated time. Chromatin-bound DNA was immunoprecipitated with the anti-E2F1 antibody. The anti- $\beta$ -actin antibody was used as a negative control. Molecular marker (M). (c) E2F1 activates miR-325 promoter activity. Cardiomyocytes were infected with the adenoviruses harboring  $\beta$ -gal or E2F1. Twenty-four hours after infection cells were transfected with the constructs of the empty vector (pGL-4.17), the wild type promoter (wt) or the promoter with mutations in the binding site (mutant), respectively. The expression levels of E2F1 were detected by immunoblot (lower panel). Firefly luciferase activities were normalized to *Renilla* luciferase. (d) A/R stimulates miR-325 promoter activity. Cardiomyocytes were transfected with the constructs of wild-type promoter (wt) or empty vector (pGL-4.17). Twenty-four hours after transfection cells were exposed to A/R. Firefly luciferase activities were normalized to *Renilla* luciferase activities. (e) E2F1 promotes miR-325 expression. Cardiomyocytes were infected with adenoviral  $\beta$ -gal or E2F1. Cells were collected at the indicated time for the analysis of E2F1 protein levels by immunoblot (lower panel), and miR-325 levels by qRT-PCR (upper panel). \* $P < 0.05$  versus control. (f) E2F1 knockout mice show a low level of miR-325. miR-325 levels by qRT-PCR (upper panel) and E2F1 levels by immunoblot (lower panel) in the hearts from E2F1 knockout mice (KO) or their wild-type littermates (WT) were analyzed.  $n = 6$ . \* $P < 0.05$  versus WT. (g) Knockdown of E2F1 inhibits autophagy and cell death. Cardiomyocytes were infected with adenoviral GFP-LC3, E2F1-siRNA or its scramble form (E2F1-sc), and then exposed to A/R. Quantitation of GFP-LC3 staining (upper panel) and cell death (middle panel) are shown. ARC and LC3 levels were analyzed by immunoblot (lower panel). The densitometric analysis of western blot of ARC and LC3-II are shown. \* $P < 0.05$  versus A/R alone. (h) miR-325 levels and autophagy are reduced in E2F1-deficient mice upon I/R. E2F1 knockout mice (KO) or wild-type mice (WT) were subjected to 45 min ischemia and 3 h reperfusion (I/R). miR-325 levels by qRT-PCR (upper panel), ARC and LC3 levels by immunoblot (lower panel) were analyzed. The densitometric analysis of western blot of ARC and LC3-II is shown. (i) E2F1-deficient mice are resistant to undergo myocardial infarction induced by I/R. E2F1 knockout mice (KO) and wild-type mice (WT) were exposed to I/R. The upper panels are representative photos of midventricular myocardial slices. The lower panel shows infarct sizes.  $n = 7$ , \* $P < 0.05$  versus WT + I/R. Bar = 2 mm

ATG12 and autophagy in pancreatic cancer cells.<sup>44</sup> Angiotensin II induces downregulation of miR-30 in cardiomyocytes, which in turn promotes myocardial hypertrophy through excessive autophagy.<sup>45</sup> Enforced expression of miR-155 can increase autophagic activity in human nasopharyngeal cancer and cervical cancer cells, whereas knockdown of miR-155 can inhibit hypoxia-induced autophagy.<sup>46</sup> Autophagy is controlled by a complex interplay between the anti- and pro-autophagic proteins,<sup>47–50</sup> and more than 800 microRNAs have been identified.<sup>51</sup> The function of miR-325 remains unknown. Our present work found that it can regulate autophagic program through targeting ARC protein. Accordingly, it can be speculated that the identification of miRNAs that regulate autophagic proteins may fill in the gap between unknown aspects of cell biology and the pathogenesis of diseases.

E2F1 is a member of E2F family that has most often been implicated in mediating apoptosis. It is reported that E2F1 expression is increased in response to myocardial ischemia/reperfusion injury, and ischemia/reperfusion injury is attenuated in E2F1 null hearts.<sup>52</sup> In present work, we investigated the role of E2F1 in autophagy upon myocardial ischemia/reperfusion injury. E2F1 knockout mice demonstrated reduced autophagy and myocardial infarction sizes upon ischemia/reperfusion injury. E2F1 participates in the autophagic pathway by regulating the expression of miR-325. Modulation of their levels may provide a new approach for tackling myocardial infarction.

## Materials and Methods

**Cells culture, anoxia/reoxygenation, apoptosis and cell death assay.** Details are in the Supplementary Methods.

**Adenoviral constructions and infection.** Mouse E2F1 cDNA and Beclin 1 were from Origene. The GFP-LC3 expression plasmid was from Cell Biolabs Inc. (San Diego, CA, USA). The adenoviruses harboring E2F1, Beclin 1 and GFP-LC3 were constructed using the Adeno-X expression system (Clontech, Mountain View, CA, USA). The adenoviruses harboring ARC or  $\beta$ -galactosidase ( $\beta$ -gal) are as we described elsewhere.<sup>53</sup> To construct adenovirus encoding miR-325, the mature miR-325 sequence was cloned into the adenovirus system according to the manufacturer's instructions.

**Generation of cardiac-specific miR-325 transgenic mice, ARC transgenic mice with 3'UTR, ARC transgenic mice without 3'UTR, ARC knockout mice and E2F1 knockout mice.** Generation of cardiac-specific miR-325 and ARC transgenic mice with 3'UTR, ARC transgenic mice without 3'UTR, ARC and E2F1 knockout mice are described in the Supplementary Methods.

**siRNA constructions of ARC, E2F1, Beclin 1 and ATG5.** ARC siRNA sequence is 5'-CTAGAAGCTGAAGCTACTG-3'; the scramble ARC siRNA sequence is 5'-AGTCAGACTGAATGCAGTC-3'. E2F1 siRNA sequence is 5'-ATC TGACCACCAACGCTT-3'; the scramble E2F1 siRNA sequence is 5'-CACTCAC GACTACGATCTA-3'. Beclin 1 siRNA sequence is 5'-GATCCTGGACCGGGTACC-3'; the scramble Beclin 1 siRNA sequence is 5'-CCTAGGCTCACGTGACGCG-3'. ATG5 siRNA sequence is 5'-GCACCTTCAGAAAGGTTATG-3'; the scramble ATG5 siRNA sequence is 5'-TATAGCGTAGCGTATGATC-3'. They were cloned into pSilencer adeno 1.0-CMV vector (Ambion, Grand Island, NY, USA) according to the manufacturer's instructions.

**Staining of autophagosomes, immunoblot, immunoprecipitation, autophagic flux.** Details are in the Supplementary Methods.

**Preparation of the luciferase construct of ARC 3'UTR and luciferase assay.** ARC 3'UTR was amplified by PCR with primer sets:

5'-AGGCCAGAATCCTTAGCTGTC-3' and 5'-CCTTCCTCTTCCTTCCTTC-3'. Mutations were generated with QuikChange II XL Site-Directed Mutagenesis Kit (Stratagene, Cambridge, MA, USA) and sequence confirmed. Wild type and mutated 3'UTRs were subcloned into the pGL3 vector (Promega, Madison, WI, USA) immediately downstream of the stop codon of the luciferase gene. Luciferase activity assay was performed as we described.<sup>54</sup>

**Target protector preparation, transfection of antagomir, constructions of mouse miR-325 promoter and its mutant.** Details are in the Supplementary Methods.

**Chromatin immunoprecipitation assay.** Chromatin immunoprecipitation (ChIP) assay was performed as we described.<sup>54</sup> In brief, cells were washed with PBS and incubated for 10 min with 1% formaldehyde at room temperature. The cross-linking was quenched with 0.1 M glycine for 5 min. Cells were washed twice with PBS and lysed for 1 h at 4 °C in a lysis buffer. The cell lysates were sonicated into chromatin fragments with an average length of 500 to 800 bp as assessed by agarose gel electrophoresis. The samples were precleared with Protein-A agarose (Roche, Mannheim, Germany) for 1 h at 4 °C on a rocking platform, and 5  $\mu$ g specific antibodies were added and rocked for overnight at 4 °C. Immunoprecipitates were captured with 10% (vol/vol) Protein-A agarose for 4 h. Before use, Protein-A agarose was blocked twice at 4 °C with salmon sperm DNA (2  $\mu$ g/ml) overnight. DNA fragments were purified with a QIAquick Spin Kit (Qiagen, Venlo, Netherlands). The purified DNA was used as a template and amplified with the following primer sets: for the analysis of E2F1 binding to the promoter region of miR-325, the oligonucleotides were as follows: forward: 5'-G CAATACACAGGTTAAATGAC-3'; reverse: 5'-GATAAGATCATTGTACTGTGG-3'.

**Quantitative reverse transcription-polymerase chain reaction.** Stem-loop quantitative reverse transcription-polymerase chain reaction (qRT-PCR) for mature miR-325 was performed as described<sup>55</sup> on an Applied Biosystems ABI Prism 7000 sequence detection system. Total RNA was extracted using Trizol reagent. After DNase I (Takara, Japan) treatment, RNA was reverse transcribed with reverse transcriptase (ReverTra Ace, Toyobo). The results of qRT-PCR were normalized to that of U6. The sequences of U6 primers were forward: 5'-GCTTCG GCAGCACATATACTAA-3'; reverse: 5'-AACGCTTCACGAATTTGCGT-3'.

**Transmission electron microscopy, ischemia/reperfusion (I/R), histology and echocardiographic assessment.** Details are in the Supplementary Methods.

**Statistical analysis.** Data are expressed as the mean  $\pm$  S.E.M. of at least three independent experiments. We evaluated the data with Student's *t* test. We used a one-way analysis of variance for multiple comparisons. A value of  $P < 0.05$  was considered significant.

**Additional experimental procedures.** These are described in the Supplementary Information.

## Conflict of Interest

The authors declare no conflict of interest.

**Acknowledgements.** This work was supported by National Natural Science Foundation of China (81270160, 31010103911), National Basic Research Program of China (973 Program, 2011CB965300), Strategic Priority Research Program of the Chinese Academy of Sciences (XDA01030000).

1. Moreau K, Ravikumar B, Renna M, Puri C, Rubinstein DC. Autophagosome precursor maturation requires homotypic fusion. *Cell* 2011; **146**: 303–317.
2. Levine B, Mizushima N, Virgin HW. Autophagy in immunity and inflammation. *Nature* 2011; **469**: 323–335.
3. Singh R, Kaushik S, Wang Y, Xiang Y, Novak I, Komatsu M et al. Autophagy regulates lipid metabolism. *Nature* 2009; **458**: 1131–1135.
4. Rabinowitz JD, White E. Autophagy and metabolism. *Science* 2011; **330**: 1344–1348.
5. Yang Z, Klionsky DJ. Eat or be eaten: A history of macroautophagy. *Nat Cell Biol* 2010; **12**: 814–822.

6. Mortensen M, Ferguson DJ, Edelmans M, Kessler B, Morten KJ, Komatsu M *et al*. Loss of autophagy in erythroid cells leads to defective removal of mitochondria and severe anemia in vivo. *Proc Natl Acad Sci USA* 2010; **107**: 832–837.
7. Pattingre S, Tassa A, Qu X, Garuti R, Liang XH, Mizushima N *et al*. Bcl-2 antiapoptotic proteins inhibit beclin 1-dependent autophagy. *Cell* 2005; **122**: 927–939.
8. Lee JH, Yu WH, Kumar A, Lee S, Mohan PS, Peterhoff CM *et al*. Lysosomal proteolysis and autophagy require presenilin 1 and are disrupted by Alzheimer-related ps1 mutations. *Cell* 2011; **141**: 1146–1158.
9. Luo J, Solimini NL, Elledge SJ. Principles of cancer therapy: Oncogene and non-oncogene addiction. *Cell* 2009; **136**: 823–837.
10. Alavez S, Vantipalli MC, Zucker DJ, Klang IM, Lithgow GJ. Amyloid-binding compounds maintain protein homeostasis during ageing and extend lifespan. *Nature* 2011; **472**: 226–229.
11. Lee Y, Ahn C, Han J, Choi H, Kim J, Yim J *et al*. The nuclear mase iii drosha initiates microRNA processing. *Nature* 2003; **425**: 415–419.
12. Bartel DP. MicroRNAs: Genomics, biogenesis, mechanism, and function. *Cell* 2004; **116**: 281–297.
13. Plasterk RH. Micro RNAs in animal development. *Cell* 2006; **124**: 877–881.
14. van Rooij E, Sutherland LB, Qi X, Richardson JA, Hill J, Olson EN. Control of stress-dependent cardiac growth and gene expression by a microRNA. *Science* 2007; **316**: 575–579.
15. Valencia-Sanchez MA, Liu J, Hannon GJ, Parker R. Control of translation and mRNA degradation by miRNAs and siRNAs. *Genes Dev* 2006; **20**: 515–524.
16. Ambros V. The functions of animal microRNAs. *Nature* 2004; **431**: 350–355.
17. Shimono Y, Zabala M, Cho RW, Lobo N, Dalerba P, Qian D *et al*. Downregulation of miRNA-200c links breast cancer stem cells with normal stem cells. *Cell* 2009; **138**: 592–603.
18. Valastyan S, Reinhardt F, Benayahu N, Calogrias D, Szasz AM, Wang ZC *et al*. A pleiotropically acting microRNA, mir-31, inhibits breast cancer metastasis. *Cell* 2009; **137**: 1032–1046.
19. Mizushima N, Sugita H, Yoshimori T, Ohsumi Y. A new protein conjugation system in human. The counterpart of the yeast apg12p conjugation system essential for autophagy. *J Biol Chem* 1998; **273**: 33889–33892.
20. Erlich S, Mizrachy L, Segev O, Lindenboim L, Zmira O, Adi-Harel S *et al*. Differential interactions between beclin 1 and bcl-2 family members. *Autophagy* 2007; **3**: 561–568.
21. Harris H, Rubinsztein DC. Control of autophagy as a therapy for neurodegenerative disease. *Nat Rev Neurol* 2011; **8**: 108–117.
22. Radoshevich L, Morrow L, Chen N, Fernandez E, Roy S, Fung C *et al*. Atg12 conjugation to atg3 regulates mitochondrial homeostasis and cell death. *Cell* 2010; **142**: 590–600.
23. Rubinstein AD, Eisenstein M, Ber Y, Bialik S, Kimchi A. The autophagy protein atg12 associates with antiapoptotic bcl-2 family members to promote mitochondrial apoptosis. *Mol Cell* 2011; **44**: 698–709.
24. Yousefi S, Perozzo R, Schmid I, Ziemiecki A, Schaffner T, Scapozza L *et al*. Calpain-mediated cleavage of atg5 switches autophagy to apoptosis. *Nat Cell Biol* 2006; **8**: 1124–1132.
25. Boya P, Gonzalez-Polo RA, Casares N, Perfettini JL, Dessen P, Larochette N *et al*. Inhibition of macroautophagy triggers apoptosis. *Mol Cell Biol* 2005; **25**: 1025–1040.
26. Frankel LB, Wen J, Lees M, Hoyer-Hansen M, Farkas T, Krogh A *et al*. MicroRNA-101 is a potent inhibitor of autophagy. *EMBO J* 2011; **30**: 4628–4641.
27. Zou Z, Wu L, Ding H, Wang Y, Zhang Y, Chen X *et al*. MicroRNA-30a sensitizes tumor cells to cis-platinum via suppressing beclin 1-mediated autophagy. *J Biol Chem* 2011; **287**: 4148–4156.
28. Xiao J, Zhu X, He B, Zhang Y, Kang B, Wang Z *et al*. Mir-204 regulates cardiomyocyte autophagy induced by ischemia-reperfusion through I $\kappa$ B- $\beta$ . *J Biomed Sci* 2011; **18**: 1–6.
29. Li YZ, Lu DY, Tan WQ, Wang JX, Li PF. P53 initiates apoptosis by transcriptionally targeting the anti-apoptotic protein arc. *Mol Cell Biol* 2008; **28**: 564–574.
30. Koseki T, Inohara N, Chen S, Nunez G. Arc, an inhibitor of apoptosis expressed in skeletal muscle and heart that interacts selectively with caspases. *Proc Natl Acad Sci USA* 1998; **95**: 5156–5160.
31. Carter BZ, Qiu YH, Zhang N, Coombes KR, Mak DH, Thomas DA *et al*. Expression of arc (apoptosis repressor with caspase recruitment domain), an antiapoptotic protein, is strongly prognostic in aml. *Blood* 2011; **117**: 780–787.
32. Mercier I, Vuolo M, Madan R, Xue X, Levalley AJ, Ashton AW *et al*. Arc, an apoptosis suppressor limited to terminally differentiated cells, is induced in human breast cancer and confers chemo- and radiation-resistance. *Cell Death Differ* 2005; **12**: 682–686.
33. Nam YJ, Mani K, Ashton AW, Peng CF, Krishnamurthy B, Hayakawa Y *et al*. Inhibition of both the extrinsic and intrinsic death pathways through nonhomotypic death-fold interactions. *Mol Cell* 2004; **15**: 901–912.
34. Yu L, Alva A, Su H, Dutt P, Freundt E, Welsh S *et al*. Regulation of an atg7-beclin 1 program of autophagic cell death by caspase-8. *Science* 2004; **304**: 1500–1502.
35. Shimizu S, Kanaseki T, Mizushima N, Mizuta T, Arakawa-Kobayashi S, Thompson CB *et al*. Role of bcl-2 family proteins in a non-apoptotic programmed cell death dependent on autophagy genes. *Nat Cell Biol* 2004; **6**: 1221–1228.
36. Ma X, Liu H, Foyil SR, Godar RJ, Weinheimer CJ, Hill JA *et al*. Impaired autophagosome clearance contributes to cardiomyocyte death in ischemia/reperfusion injury. *Circulation* 2012; **125**: 3170–3181.
37. Levine B, Yuan J. Autophagy in cell death: An innocent convict? *J Clin Invest* 2005; **115**: 2679–2688.
38. Gustafsson AB, Tsai JG, Logue SE, Crow MT, Gottlieb RA. Apoptosis repressor with caspase recruitment domain protects against cell death by interfering with bax activation. *J Biol Chem* 2004; **279**: 21233–21238.
39. Ekhterae D, Lin Z, Lundberg MS, Crow MT, Brosius FC, Nunez G. Arc inhibits cytochrome c release from mitochondria and protects against hypoxia-induced apoptosis in heart-derived h9c2 cells. *Circ Res* 1999; **85**: e70–e77.
40. Neuss M, Monticone R, Lundberg MS, Chesley AT, Fleck E, Crow MT. The apoptotic regulatory protein arc (apoptosis repressor with caspase recruitment domain) prevents oxidant stress-mediated cell death by preserving mitochondrial function. *J Biol Chem* 2001; **276**: 33915–33922.
41. Gustafsson AB, Sayen MR, Williams SD, Crow MT, Gottlieb RA. Tat protein transduction into isolated perfused hearts: Tat-apoptosis repressor with caspase recruitment domain is cardioprotective. *Circulation* 2002; **106**: 735–739.
42. Chhabra R, Adlakha YK, Hariharan M, Scaria V, Saini N. Upregulation of mir-23a-27a-24-2 cluster induces caspase-dependent and -independent apoptosis in human embryonic kidney cells. *PLoS One* 2009; **4**: e5848.
43. Su H, Yang JR, Xu T, Huang J, Xu L, Yuan Y *et al*. MicroRNA-101, down-regulated in hepatocellular carcinoma, promotes apoptosis and suppresses tumorigenicity. *Cancer Res* 2009; **69**: 1135–1142.
44. Wang P, Zhang J, Zhang L, Zhu Z, Fan J, Chen L *et al*. MicroRNA 23b regulates autophagy associated with radioresistance of pancreatic cancer cells. *Gastroenterology* 2013; **145**: 1133–1143; e1112.
45. Pan W, Zhong Y, Cheng C, Liu B, Wang L, Li A *et al*. Mir-30-regulated autophagy mediates angiotensin II-induced myocardial hypertrophy. *PLoS One* 2013; **8**: e53950.
46. Wan G, Xie W, Liu Z, Xu W, Lao Y, Huang N *et al*. Hypoxia-induced is a potent autophagy inducer by targeting multiple players in the mtor pathway. *Autophagy* 2013; **10**: 70–79.
47. McPhee CK, Logan MA, Freeman MR, Baehrecke EH. Activation of autophagy during cell death requires the engulfment receptor draper. *Nature* 2010; **465**: 1093–1096.
48. Yu L, McPhee CK, Zheng L, Mardones GA, Rong Y, Peng J *et al*. Termination of autophagy and reformation of lysosomes regulated by mtor. *Nature* 2010; **465**: 942–946.
49. Nishida Y, Arakawa S, Fujitani K, Yamaguchi H, Mizuta T, Kanaseki T *et al*. Discovery of atg5/atg7-independent alternative macroautophagy. *Nature* 2009; **461**: 654–658.
50. Yang Q, She H, Gearing M, Colla E, Lee M, Shacka JJ *et al*. Regulation of neuronal survival factor mef2d by chaperone-mediated autophagy. *Science* 2009; **323**: 124–127.
51. Djuranovic S, Nahvi A, Green R. A parsimonious model for gene regulation by miRNAs. *Science* 2011; **331**: 550–553.
52. Angelis E, Zhao P, Zhang R, Goldhaber JL, MacLellan WR. The role of e2f-1 and downstream target genes in mediating ischemia/reperfusion injury in vivo. *J Mol Cell Cardiol* 2011; **51**: 919–926.
53. Murtaza I, Wang HX, Feng X, Alenina N, Bader M, Prabhakar BS *et al*. Down-regulation of catalase and oxidative modification of protein kinase c $\kappa$ 2 lead to the failure of apoptosis repressor with caspase recruitment domain to inhibit cardiomyocyte hypertrophy. *J Biol Chem* 2008; **283**: 5996–6004.
54. Wang K, Long B, Zhou J, Li PF. Mir-9 and nfat3 regulate myocardin in cardiac hypertrophy. *J Biol Chem* 2010; **285**: 11903–11912.
55. Chen C, Ridzon DA, Broomer AJ, Zhou Z, Lee DH, Nguyen JT *et al*. Real-time quantification of microRNAs by stem-loop rt-pcr. *Nucleic Acids Res* 2005; **33**: e179.

Supplementary Information accompanies this paper on Cell Death and Differentiation website (<http://www.nature.com/cdd>)